Anal. Bioanal. Electrochem., Vol. 16, No. 6, 2024, 537-558
https://www.doi.org/10.22034/abec.2024.714077

Analytical & Bioanalytical Electrochemistry

Full Paper

Synthesis, Structural Determination, Electrochemical Investigation of Metal Complexes of Novel 4-[3-Hydroxypyridin-2-yl)diazenyl]-5-methyl-2-phenyl-2,4-dihydro-3H-pyrazol-3-one; Biological Evaluations

H.A. Anilkumara,[1] G. Krishnamurthy,[1,*] M.N. Manjunatha,[2] Prabhakar Chavan,[1] Malathesh Pari,[1] N. Ranjitha,[1] and Fasiulla Khan[3]

[1]*Department of P.G. Studies and Research in Chemistry, Sahyadri Science College, Kuvempu University, Shivamogga -577 203, Karnataka, India*
[2]*Department of Chemistry, M S Ramaiah Institute of Technology, Bangalore-560054, Karnataka, India*
[3]*Department of Chemistry, Manipal University, Manipal – 576104, Karnataka, India*

*Corresponding Author, Tel.: +234 8060123864
E-Mail: gkmnaiksahyadri@gmail.com

Received: 31 January 2024 / Received in revised form: 1 June 2024 / Accepted: 7 June 2024 / Published online: 30 June 2024

Abstract- The pyrazole derivatives and its metal complexes are considered to be pharmacologically significant with a variety of pharmacological applications. The present investigation highlights the synthesis of pyrazole based novel ligand, 4-[(*E*)-(3-hydroxypyridin-2-yl)diazenyl]-5-methyl-2-phenyl-2,4-dihydro-3*H*-pyrazol-3-one (PDP) and its Co(II), Ni(II), Cu(II) complexes. The structure of the synthesized compounds has been evaluated using various physicochemical and spectroscopic techniques. Cyclic Voltammetry (CV) results are used to confirm the electrocatalytic ability of the modified electrode, $[Co(PDP)_2]Cl_2.2H_2O$/GCE for the detection of Folic acid (FA) at different concentrations. The CV results displayed good electro-catalytic activity with 10-120 μML^{-1} with limits of detection (LOD) of 0.0666 μML^{-1}. This electrode has a sensitivity of 2.8784 $\mu A \mu M^{-1} cm^{-2}$ for FA. The bio-efficacy of the synthesized ligand and its complexes have been evaluated against the bacteria (S.aures and E.coli) and fungal (A.flavus and P.anomala) strains using standard method. Antidiabetic study on two different enzymes, α- amylase and α-Glucosidase indicating excellent inhibition by the metal complexes having the maximum IC_{50} Value of 105.34 for α-amylase and 107.15 mg/mL for α- Glucosidase.

Keywords- Azo-dye; Metal complexes; Cyclic voltammetry; Antidiabetics; Folic acid

1. INTRODUCTION

Azo-dye molecules having (-N=N-) group that can serve as ligands in coordination chemistry. These ligands are often used in the purification of biomolecules, such as proteins and enzymes. The metal complexes of ligand which containing azo group play an important role in the advancement of coordination chemistry [1-2]. The study of coordination chemistry of azo-dye metal complexes involves intereseting bonding interactions, spectroscopic properties and their reactivity which contributes for the development of new materials and technologies [3-4]. The pyrazole derivatives and its metal complexes are considered as a pharmacologically active because of their antitumor [5], antiulcer [6], antifungal and antibacterial [7-9], antihelmintic [10], anti-inflammatory [11], anticonvulsant [12], antitubercular [13], antidepressant [14], antihypertensive [15], anticoagulant [16], and antiviral [17] activities. Transition metals such as Co, Cu and Ni found in biological system and can catalyse many biological functions. Transition metal ions in their complexes show variable oxidation states, redox behavior and acquire different structure. This structural change makes them to have important psychological functions. During the previous decades, there has been a lot of interest in the use of transition metal complexes for electrochemical studies and applied for the electrochemical detection of a number of biologically important chemicals [18-20].

Cyclic voltammetry (CV) is an important electrochemical technique used to investigate the redox properties of compounds. It involves cycling the potential of a working electrode linearly with time and measure the resulting current to analyze the electrochemical behavior of analytes. In electro-oxidation, CV can reveal information about the oxidation states, kinetic parameters, and reaction mechanisms by observing the anodic peaks. Conversely, electro-reduction helps to identify cathodic reactions and reduction potentials. This method is more precisely valuable due to its ability to provide rapid and detailed insights into both reversible and irreversible electrochemical processes. Therefore, it is essential for studying reaction intermediates, electrode surface phenomena, and the overall redox stability of compounds [21-24].

Folic acid found mainly in dark green leaves, beans, peas and nuts. It is an essential component of prenatal vitamins and is in many fortified foods such as cereals and pastas. It has excellent curative properties for treats low level vitamin B9 in our body that helps to make red blood cells and play an important role in maintaining brain health [25-26]. Deficiency of folic acid in animals can lead to various health issues, including anemia, poor growth, reproductive problems etc., and in human, its deficiency leads to several health issues, including megaloblastic anemia, that causes fatigue and weakness. Folic acid is very crucial for DNA synthesis and repair and its deficiency also contribute to neutral tube defects during early pregnancy. Therefore, the detection of folic acid in biological system is an important cause of concern. In the present study Folic acid can be detected by a simple and easy method like cyclic voltammetry (CV) because, it undergo redox reactions [27-28].

The research work concern to synthesis of transition metal complexes of novel heterocycles and investigation of biological activity and electrochemical detection of different vital chemicals have been done in our laboratory [29]. In continuation, the synthesis of 4-[(*E*)-(3-hydroxypyridin-2-yl)diazenyl]-5-methyl-2-phenyl-2,4-dihydro-3*H*-pyrazol-3-one (PDP) and its Co(II), Ni(II) and Cu(II) complexes their characterization by various spectral method have been done. Further, the electrochemical detection of folic acid and biological evaluation like antidiabitic, antioxidant activity and antibacterial activity of the ligand and its complexes.

2. EXPERIMENTAL SECTION

2.1. Preparation of Specimen

2-Amino-3-hydroxypyridine, Phenylhydrazone, Ethylacetoacetate, $NaNO_2$ purchased from sd-fine chemicals. Ethanol was purified using literature method [30]. The laboratory grade metal salts purchased from Sigma Aldrich. These chemicals as such used to prepare the ligand and their metal complexes without further purification. The Innovative DTC-967A digital melting point analyzer was utilized to determine the melting point. The carbon, hydrogen, and nitrogen elemental analysis were recorded by Perkin-Elmer 2400 series II CNS analyzer. IR Spectra were determined by FTIR spectroscopy IR Spirit Shimadzu serial no; A224159 (Made in Japan) at Sahyadri Science College, Shivamogga, Karnataka, India. Spectrometer with KBr pellets which were made by using hydrolic press and spectra were recorded in the range 250-4500 cm^{-1}. Absorbance is measured with a Systronics UV–Vis spectrometer 119 at Sahyadri science college Shivamogga. Using TMS as the internal standard, the ^1H NMR spectrum was captured using a Bruker analyzer operating at 400 MHz in DMSO-d6 at Mysore University, Mysore, India. The synthesized compounds LC-MS compositions were identified by using MS make made in USA, model Acquity UPLC at Mysore. The Rigaku Miniflex 600 apparatus was used for the analysis of the PX-ray parameters. The SDT Q600 V20.9 was used for the TGA/DTA measurements of the metal complexes, at SAIF, Karnataka University, Dharwad. The thermogram was recorded by heating at a rate of 20 ℃/min from atmospheric temperature to 850^{o}C. Cyclic voltammetry study was carried out using an electrochemical analyzer manufactured in the United States by CH- instrument at the Sahyadri Science College in Shivamogga, Karnataka, India.

2.2. Synthesis of the azo-dye Ligand

Azo-dye ligand has been synthesized in two steps. In the first step, phenylhydrazone (5 mmol, 10 mL in 15 mL ethanol), ethylacetoacetate (5 mmol, 13 mL) and a pinch of KOH were dissolved in an ethanolic solution. The reaction mixture was stirred for about an hour at 0–10 ^{o}C. Then the solution was refluxed for about 8-10 hrs at 70 ℃. When a light yellow precipitate formed, it was poured into to the crushed ice and neutralized it with diluted or 1:1 acetic acid.

The resulting compound was filtered, washed with distilled water, Recrystallized using ethanol and then dried.

The coupling agent, 2-amino-3-hydroxypyridine was dissolved in the solution of $NaNO_2$ in HCl (10 mmol, 1:1 ratio) and added to an alkaline solution of 5-methyl-2-phenyl-1,2 dihydro-3H-pyrazole-3-one (5 mmol, 0.6 g) (1.4 g of NaOH in 15 mL of water). The resulting mixture was stirred continuously for about 03 hrs in the temperature range 0-5 °C. The progress of the reaction was monitored by TLC and the green colored solid formed was collected. The product formed was recrystallized form the ethanol. Yield 72%. The Scheme 1 illustrates the path of ligand synthesis.

Step 1: Synthesis of 5-methyl-2-phenyl-1,2 dihydro-3H-pyrazole-3-one

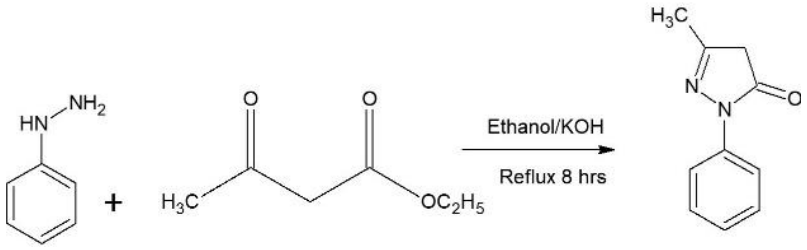

Step 2:

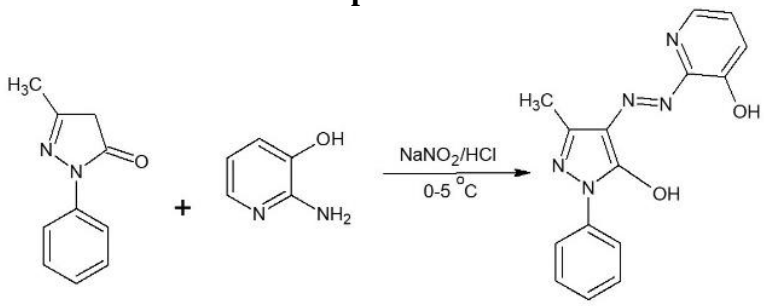

Scheme 1. Schematic representation of synthesis of 4-[(E)-(3-hydroxypyridin-2-yl)diazenyl]-5-methyl-2-phenyl-2,4-dihydro-3H-pyrazol-3-one (PDP)

2.3. General procedure for synthesis of metal complexes

The hot absolute ethanolic solution (10mL) of ligand (PDP) (0.002 mole) was stirred continuously for about 5 min. Chloride of metals (Co, Ni and Cu) (0.001 mole) dissolved in 10 mL absolute ethanol was added into the ligand solution (one metal chloride at each time). The resulting solution was then stirred with reflux for an additional 5 hrs. After attaining the room temperature, the excess solvent was removed by evaporation. The reaction product was allowed to cool at room temperature. The colored precipitate was produced, which was then filtered, washed with distilled water and ethanol, and dried in a vacuum desiccator over anhydrous calcium chloride. Scheme 2 illustrates the synthetic route of metal compounds and their proposed structure (Yield 69-70%) [31-33].

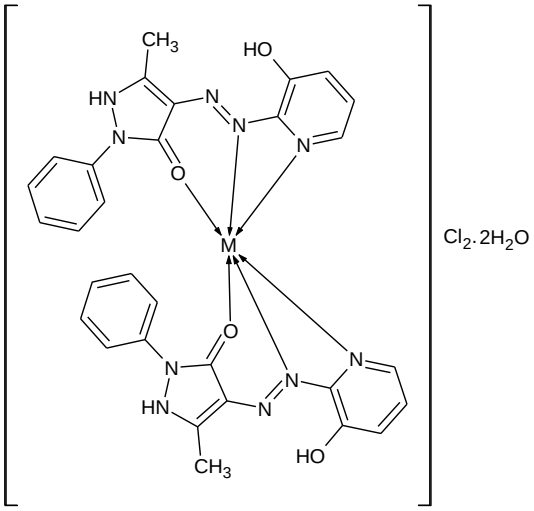

M=Co^{+2}, Ni^{+2} and Cu^{+2}

Scheme 2. Synthesis of Metal complexes

2.4. Electrochemical determination

Tri-electrode systems with a glassy carbon electrode (GCE) as the working electrode, platinum wire as the counter, and an Ag/AgCl reference electrode were used in electrochemical experiments on a CH instrument of type $CH_{I6}0_8D$ (USA). By using the synthesized metal complexes the modified electrode was prepared and the electrocatalytic activity was determined and this modified electrode was used detect the presence of folic acid in the solution at different concentrations for various concentrations of folic acid (FA) [34,35].

2.5. Biological screening

2.5.1. Antibacterial screening

The agar-well diffusion method was used to examine the antibacterial activity of PDP and its metal complexes against gram-positive bacteria such as Staphylococcus aureus (MTCC-7443) and Baccilus licheniformis (MTCC-2465) [36], as well as gram-negative bacteria such as Acetobacter Sp (MTTC-3245) and Pseudomonas aeruginosa (MTTC-1688). The inoculums were increased with clean saline solution to nearly 5x105CFU/mL. The majority of the synthesized compounds were loaded into five different wells at concentrations varying from 100 to 200 g using DMSO as a stock solution at a concentration of 10 mg/mL. (Chloramphenicol has been used as reference standard). Following 24-hrs of incubation time for bacteria at 37°C, the distance across the inhibition zone (mm) was measured, and the relative percent inhibition against the reference drug was calculated using the formula provided in the literature [37].

2.5.2. Antifungal screening

The agar-well diffusion technique was used to assess antifungal activity of the synthesized compounds against Penicillium expansum (MTCC-8241) and Aspergillus flavus (MTCC-9606) [38]. The stock solution containing 10 mg/mL of synthesized substances was diluted in DMSO at a concentration and labeled in five distinct concentration ranges of 100 to 200 mg for five separate wells. (Fluconazole has been used as reference standard). After 48-hrs of incubation period the zone of inhibition around the wells was recorded.

2.5.3. Antidiabetic activity

2.5.3.1. Inhibitory activity against α-Amylase

The ability of synthesized compounds to inhibit α-amylase were tested in accordance with instructions described by Poovitha et.al [39] Porcine pancreatic α-amylase was dissolved in 0.1 M phosphate buffered saline, pH 6.9, at a concentration of 3 units/mL. The enzyme was pre-incubated with the various sample concentrations (0-125 g/mL) for 10 min at 37°C. The incubation medium substrate (0.1% starch) was added to start the reaction. Adding 250 mL of the dinitro salicylic (DNS) reagent (1% 3, 5-dinitrosalicylic acid, 0.2% phenol, 0.05% Na_2SO3, and 1% NaOH in aqueous solution) stopped the reaction after it had been incubating for 10 minutes. By placing the reaction mixture in a 10-minute immersion in hot water, the reaction was stopped. 250 L of a 40% potassium sodium tartrate solution was then introduced. The absorbance at 540 nm was measured after cooling to room temperature in a cold-water bath. (OD of blank - OD of test/OD of Blank) *100 was used to compute the percentage of inhibition, and the results were represented as IC_{50} values in comparison to acarbose as a positive control [40].

2.5.3.2. Inhibitory activity against α-Glucosidase

The procedure described in as used to assess the ability of synthesized compounds to block -glucosidase. Alpha-glucosidase was dissolved in phosphate buffer (50 mM, pH 6.9) and pre-treated individually with a range of sample concentrations (0-125 g/mL) for 10 min at 37°C. 50 mL of 5 mM p-nitrophenyl-D glucopyranoside in phosphate buffer was added to start the reaction. For 30 minutes, the enzyme reaction was conducted at 37 °C. After the addition of Na_2CO_3 (1 M) read the absorption at 405 nm stopped the process. (OD of blank-OD of test/OD of Blank) *100 was used to compute the percentage of inhibition, and the results were represented as IC50 values in comparison to acarbose as a positive control [41].

3. RESULTS AND DISCUSSION

3.1. Chemical analysis

Newly synthesized azo-dye ligand and its complexes were stable at room temperature and are soluble in common organic solvents like ethanol, methanol and chloroform. The molar

conductivity values calculated at room temperature in 0.001 M solution of DMF. Metal complexes were found to have conductivity values between 08 and 15 $ohm^{-1}cm^2mol^{-1}$, indicating of uni-bivant behavior [42]. The elemental analysis data agrees fairly well with the calculated values and are collected in Table 1.

Table 1. Physical properties and analytical data of the PDP and its metal complexes

Comp. No. and Colour	Mol. Wt.	Yield (%)	CHN Analysis Found (Calculated) (%)				Molar Conductance ($ohm^{-1}cm^2mol^{-1}$)	M.P. (^oC)
			M	C	N	H		
L (PDP) Green	295.29	72	-	65.23 (64.99)	20.34 (19.55)	4.89 (4.11)	-	229
$[Co(PDP)_2]Cl_2.2H_2O$ Brown	649.52	69	8.24 (8.04)	57.66 (56.16)	16.33 (15.87)	4.43 (4.10)	119	263
$[Ni(PDP)_2]Cl_2.2H_2O$ Light green	649.28	68	9.79 (9.11)	60.62 (60.02)	17.65 (16.98)	5.66 (5.20)	116	259
$[Cu(PDP)_2]Cl_2.2H_2O$ Dark green	654.13	70	9.12 (9.07)	54.44 (53.55)	16.43 (15.76)	4.30 (4.02)	118	265

3.2. ^1H and ^{13}C NMR spectral studies

^1H NMR spectrum of PDP (Figure 1) appeared a sharp singlet at 5.35 ppm caused by -OH proton (S,1H, OH) and NH appeared at 3.45 ppm (S,1H, NH). The aromatic ring protons appeared as multiplets in 7.85–7.00 ppm region. Another singlet appeared for proton of CH_3 in aliphatic group between 2-2.5 ppm. The absence of O-H signal of moiety pyrazole group ^1H NMR spectrum of the ligand is evidence that the keto form exists in place of the enol form [43]. The absence of a proton as a result of partial oxidation or interaction between protons and the solvent DMSO.

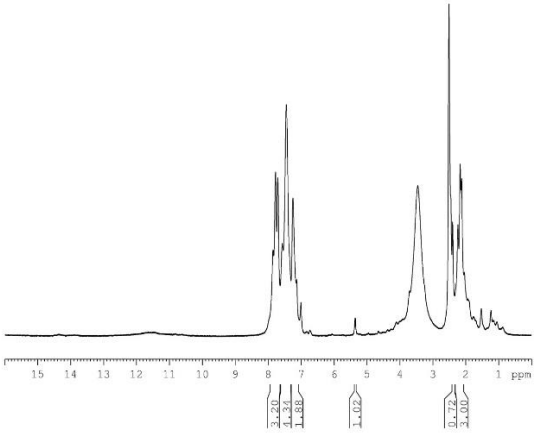

Figure 1. ^1H NMR spectrum of PDP

The carbon next to the hydroxyl group of the ligand in ^{13}C NMR spectrum showed a signal at 159.91 ppm and 160.7 ppm due to carbonyl group C=O. The carbon atoms next to the diazo group (N=N) exhibit signal at 126.10 ppm. The signal at 17.68 ppm is due to carbon of methyl (CH_3-C) and the peaks at 112.44 and 101.78 ppm corresponds to resonance of aromatic carbon. Figure are showed in supplementary Figure S1.

3.3. Mass spectral studies

The mass spectra of the PDP a well-defined molecular ion peak at m/z 295.29, which corresponds to its molecular mass is showed in supplementary Figure S2. The molecular ion peak of the Co(II), Ni(II) and Cu(II) complexes were found at m/z of 650.70 (cal 649.52), 650.55 (cal 649.28) and 655.65 (cal 654.13), which correspond to a stoichiometric ratio of 1:2 (M:L). Furthermore, the ligand and its metal complexes match their proposed molecular structures. The metal complexes mass spectra are given in supplementary information file (Figures S3, S4, S5).

3.4. IR spectral studies

The infrared spectral data of PDP and its metal complexes were recorded as KBr pellets in the region 4000-350 cm^{-1} are presented in supplementary Table S1 and Figure S6. In the IR spectra of the PDP, the absorption band due to -OH stretching vibrations were observed at 3416 cm^{-1}. The -OH stretching appeared in the same region in all the complexes expecting slight shift to the lower frequencies by 50-40 cm^{-1}. The stretching frequency due to azo group (-N=N) was observed at 1368 cm^{-1}. The azo group is shifted to higher frequency by 30-50 cm^{-1} in the metal complexes appeared at 1390 to 1394 cm^{-1} indicating the participation of one of the azo nitrogen atoms in coordination with metal ion. The ν(C=N) stretching observed at 1615 cm^{-1} has no shift in the spectra of all the complexes indicating non – involvement of C=N in the coordination. The carbonyl group (C=O) was observed at 1745 cm^{-1} is shifted to higher frequency by 30-50 cm^{-1} in the metal complexes. The participation of the ligand in the coordination with metal ion is observed through -N=N- group as it is evidenced by the appearance of new bands in the region 436-428 cm^{-1} for ν(M-N) vibrations similarly, new bands within the region 530-544 cm^{-1} are assigned to ν(M-O) mode of bonding.

3.5. Electronic spectra and magnetic moment studies

The electronic spectra of the synthesized azo dye ligand and its metal complexes are displayed in supplementary Figure S7. and the values are given in supplementary Table S2. PDP, a green colored compound showed an absorption band at 28,571 cm^{-1} is which assigned to the charge transfer transition. The brown colored $[Co(PDP)_2]Cl_2.2H_2O$ displayed three bands at 14,925, 16,666 and 22,222 cm^{-1} which are due to $^4T_{1g}(F) \rightarrow {}^4T_{2g}(F)$ (ν_1), $^4T_{1g}(F) \rightarrow {}^4A_{2g}(F)$ (ν_2)

and $^4T_{1g}(F) \rightarrow {}^4T_{1g}(F)$ (ν_3) transitions respectively. The magnetic moment of 4.73 and the electronic transitions suggest octahedral geometry around the Co(II). The $[Ni(PDP)_2]Cl_2.2H_2O$ complex showed a transition at 12,658 cm^{-1} due to $^3A_{2g}(F) \rightarrow {}^3T_{2g}(F)$ (ν_1) and the second transition $^3A_{2g}(F) \rightarrow {}^3T_{1g}(F)$ (ν_2) has occurred at 15,625 cm^{-1}. The third transition appeared at 22,222 cm^{-1} ascribed to $^3A_{2g}(F) \rightarrow {}^3T_{1g}(F)$ (ν_3). In addition the observed magnetic moment value 2.75 BM indicate octahedral geometry. The $[Cu(PDP)_2]Cl_2.2H_2O$ complex showed a broad band at 24,390 cm^{-1} due to $^2E_g(F) \rightarrow {}^2T_{2g}(F)$ (ν_1) for octahedral geometry. The magnetic moment of 1.70 BM.

3.6. X-ray diffraction studies

The metal (II) complexes were subjected to X-ray diffraction, which was recorded at 2θ = 0-80°, to learn more about their structural information and the data are listed in supplementary Figure S8 and Tables S3a S3b and S3c. For, $[Co(PDP)_2]Cl_2.2H_2O$, unit cell parameters are a = 4.9890 Å, b = 6.9780 Å, c = 17.0620 Å and the density 10.78 g/cm^3. In the $[Ni(PDP)_2]Cl_2.2H_2O$, unit cell parameters are a = 25.080 Å, b = 22.909 Å, c = 12.760 Å and density 9.20 g/cm^3. For, $[Cu(PDP)_2]Cl_2.2H_2O$, unit cell parameters are a = 11.210 Å, b = 14.150 Å, c = 10.021 Å and density 9.45 g/cm^3. Indicating that the complexes are in a crystalline phase [44].

3.7. SEM and EDX spectra

The Scanning Electron Microscopy (SEM) and Energy Dispersive X-ray analysis (EDX) These studies provided a better understanding about the surface characteristics and the chemical composition of the sample materials. PDP and its metal complexes are illustrated in supplementary Figure S9. In the SEM image of PDP the structure appears granular and distorted, while the $[Co(PDP)_2]Cl_2.2H_2O$ and $[Cu(PDP)_2]Cl_2.2H_2O$ exhibits a needle-like morphplogy. The $[Ni(PDP)_2]Cl_2.2H_2O$ displayed a fragmented and broken bar like structure. The EDX analysis confirmed that in PDP, carbon, oxygen and nitrogen in PDP and the metals such as cobalt, nickel and copper signal obtained in their respective complexes along with the ligand elements.

3.8. Thermal analysis

Thermogravimetric analysis was used to determine the thermal disintegration of Co(II) , Ni(II) and Cu(II) complexes in the temperature range of 25-800 ^oC. Table 2 is a results of the thermal stability data. The thermogravimetric technique results made it abundantly clear that the disintegration of the complexes occur in three stages [45,46]. The temperature versus percentage graph showed the weight loss which is represented in Figure 2.

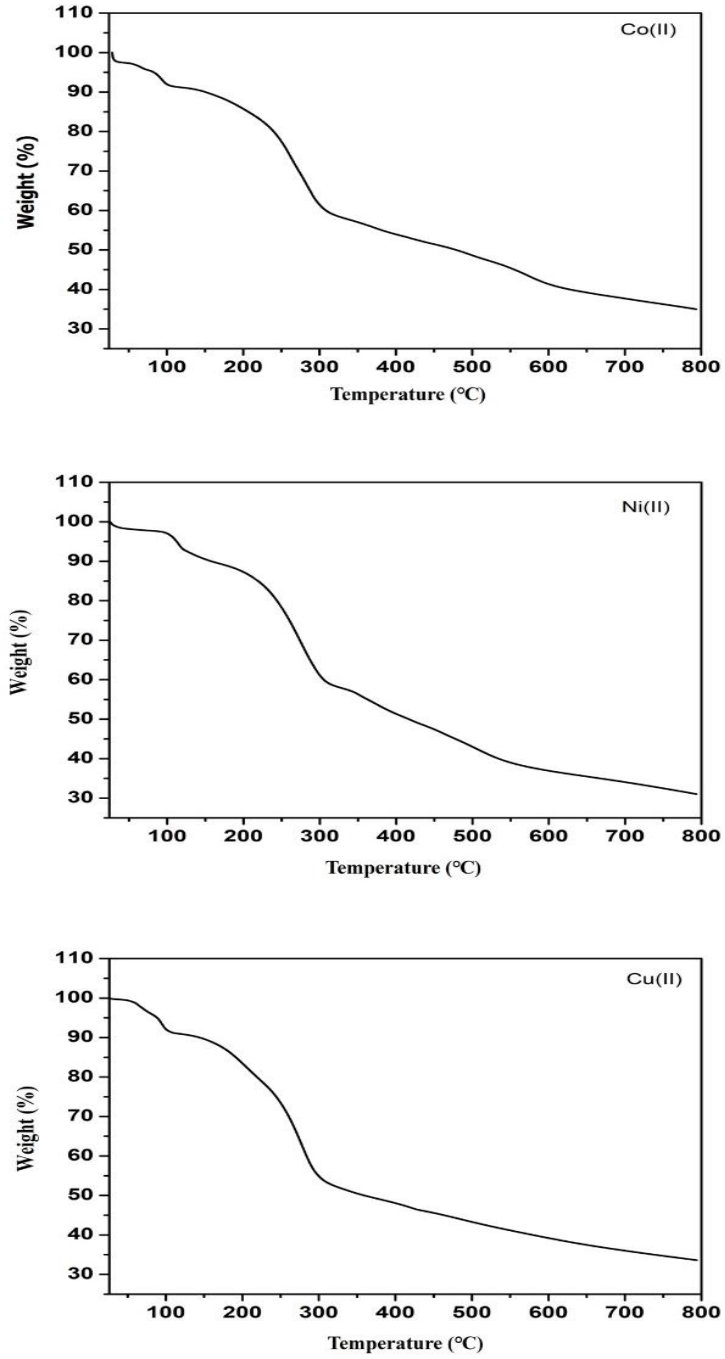

Figure 2. Thermal analytical curve of (a) $[Co(PDP)_2]Cl_2.2H_2O$ (b) $[Ni(PDP)_2]Cl_2.2H_2O$ (c) $[Cu(PDP)_2]Cl_2.2H_2O$

The $[Co(PDP)_2]Cl_2.2H_2O$ represent three stages of degradation. The thermogram of $[Co(PDP)_2]Cl_2.2H_2O$ complex showed first stage of degradation with a mass loss of 5.13% (cal: 5.50%) indicating that weight loss of $2H_2O$ in the temperature range 56-85^oC. In the second stage, the weight loss of 42.27% (cal: 43.55%) has occurred in the range 85-302^oC due to removal of organic molecules and pyridine moiety. Third stage resulted in weight loss of 23.07% (cal: 24.22%) due to degradation of pyrazole ring. Finally CoO as residue from temperature range 302-705 ^oC. $[Ni(PDP)_2]Cl_2.2H_2O$ degraded in three stages , in the region 28-

104^{o}C was about 4.22% (cal:4.50%) which corresponds to the weight loss of two water molecules. The second stage represents weight loss found 48.11% (cal: 49.70%) due to the degradation of organic molecules with pyridine moiety. Third stage resulted in weight loss found 28.83% (cal:29.90%) due to the loss of pyrazole moiety from temperature range 353-722^{o}C, NiO was expected as residue. The degradation step of $[Cu(PDP)_2]Cl_2.2H_2O$ involves in three stages. The first stage occur in temperature range 56-89 ^{o}C due to the weight loss of $2H_2O$ molecule 5.04% (cal: 5.50%). The second stage temperature range 89-297 ^{o}C resulted in a weight loss of 46.87% (cal: 48.50%) elimination of organic molecules with pyridine moiety. The third stage of degradation due to the removal of pyrazole ring in the temperature range 297-702 ^{o}C weight loss 28.90% (cal: 29.50%) CuO residue remaining as stable.

Table 2. Thermal degradation data of metal complexes

Comp. No.	Decomposition stages	Decomposition temperature range ^{o}C	Assignment	Loss of mass in (%)	Residue species
$[Co(PDP)_2]Cl_2.2H_2O$	1st	56-85	$2H_2O$	5.13	CoO
	2nd	85-302	$C_{11}H_{17}N_6$	42.27	
	3rd	302-705	$C_{19}H_7N_4O_2$	23.07	
$[Ni(PDP)_2]Cl_2.2H_2O$	1st	50-104	$2H_2O$	4.22	NiO
	2nd	104-353	$C_{11}H_{17}N_6$	48.11	
	3rd	353-722	$C_{19}H_7N_4O_2$	28.83	
$[Cu(PDP)_2]Cl_2.2H_2O$	1st	56-89	$2H_2O$	5.04	CuO
	2nd	89-297	$C_{11}H_{17}N_6$	46.87	
	3rd	297-702	$C_{19}H_7N_4O_2$	28.90	

3.9. Electrochemical studies

3.9.1. Electrochemical investigation

The oxidation potential of Folic acid (FA) in phosphate buffered solutions at pH 7 with bare GCE (glassy carbon electrode) and with modified GCE was investigated to check the electrochemical sensing act for the CV of (a) bare GCE and (b) $[Co(PDP)_2]Cl_2.2H_2O$/GCE, a modified electrodes in 05 μML^{-1} concentration for FA. As per literature reports, the modified electrodes are recognized for exhibiting enhanced activity in both physicochemical and electrochemical dimensions. Therefore, in the present investigation a modified GCE, $[Co(PDP)_2]Cl_2.2H_2O$/GCE has been prepared by drop- coated method and used to determine the electrochemical behaviors which exhibited a strong peak current as showed in Figure 3.

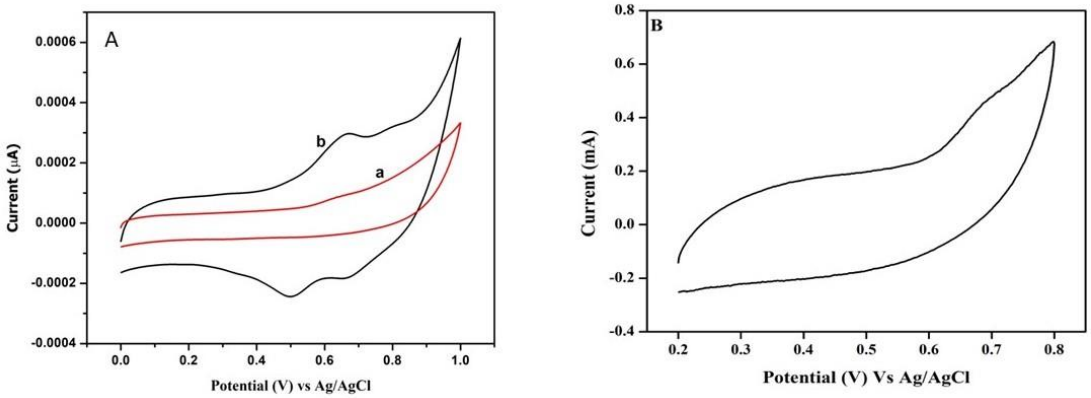

Figure 3. Cyclic voltammogram of A) (a) GCE (bare electrode); (b) $[Co(PDP)_2]Cl_2.2H_2O$/ GCE with FA 05 μML^{-1} at a scan rate = 50 mV/s; B) Modified electrode in the blank solution

3.9.2. Electrochemical detection of different concentration of Folic acid (FA)

To get $[Co(PDP)_2]Cl_2.2H_2O$/GCE, a saturated solution of $[Co(PDP)_2]2H_2O$ in DMF was drop-coated over a glassy carbon electrode. It was observed that the electrocatalytic performance of this electrode was very good. The electrocatalytic behavior of FA at various concentrations of 05 to 40 μML^{-1} in phosphate buffer solution at pH 7 is depicted in the graph, Figure 4. It was observed that FA reacted linearly to reduction current (I_p), with the linear equation Y= (FA) to 0.04014 + 2.891 indicating a satisfactory linear response with an R^2 value of 0.9958. The addition of different concentrations of FA led to an increase in the electrocatalytic peak current. The electro-reduction peaks of FA were seen close to the metal ions during the electro catalysis process.

The shift in oxidation peak in cyclic voltammetry (CV) can occur due to various factors related to the electrochemical system and experiment conditions. Here are some common reasons for the shift [47,48].

1. Concentration of the analyte can alter, the position of the oxidation peak. Higher concentrations may lead to a peak shift due to increased interactions among the molecules.
2. pH of the solution may also contribute for the shift due to migration of ions.
3. Reaction mechanism involvement of different intermediates changes in the number of electron transfer may cause shifting of the peak.
4. The other factors also influence to some extent which are scan rate and temperature, faster scan rate shifts the higher peak. Similarly, temperature can affect the reaction kinetics and diffusion rate.

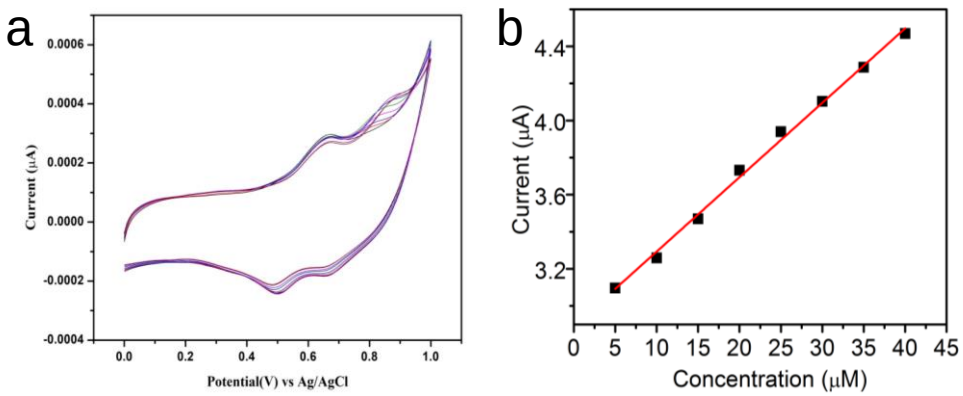

Figure 4. Cyclic voltammogram of $[Co(PDP)_2]Cl_2.2H_2O$/GCE at (a) different concentration FA 05-40 μML^{-1} (b) calibration graph of peak current vs. concentration FA in PBS pH 7 at scan rate 50 mV/s

3.9.2. Effect of scan rate

Using pH 7 buffer solution and an increase in scan rate from 10 to 90 mV/s, the effect of scan rate on $[Co(PDP)_2]Cl_2.2H_2O$/GCE was examined (Figure 5) [49]. The graph depicts an increase in scan rate as peak current increases. According to the regression equation I(A) = 35.72(FA) + 0.985 V and correlation coefficient R^2=0.9953, the current intensity was linearly related to scan rate in the region of 10 to 90 mV/s, and the electrochemical reaction was regulated by adsorption. The limit of detection (LOD) of 1.666 μML^{-1} and sensitivity of 350720 $\mu A \mu M^{-1} cm^{-2}$ of the $[Co(PDP)_2]Cl_2.2H_2O$/GCE demonstrate its suitability for monitoring FA.

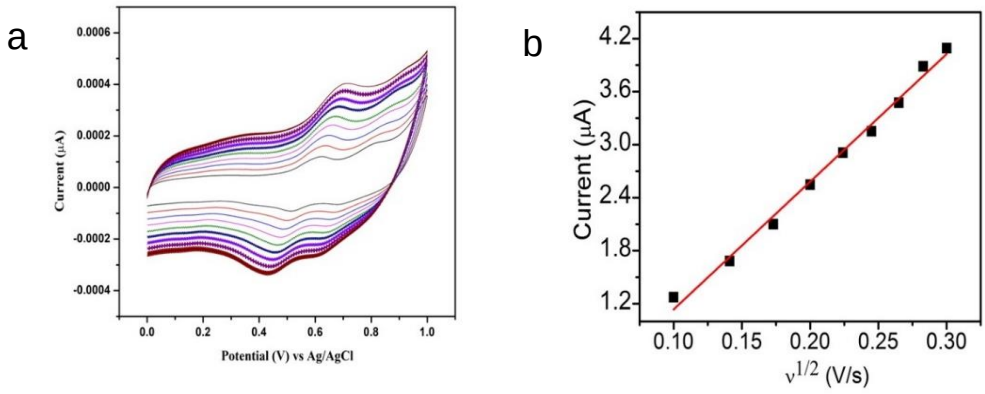

Figure 5. (a) CVs plot of different scan rate of FA; scan rate 10-90 mV/s; (b) Calibration graph of square root of scan rate vs. peak current

3.9.3. Different pH

The pH study was conducted in three distinct pH-buffered media, which enhanced the stability and efficiency of the electrochemical analysis. The supporting electrolyte plays a crucial role in the electrochemical measurements of electroactive molecules. The relationship

between E_{pa} and various pH levels is depicted in supplementary Figure S10. The influence of pH (4, 7, and 9) on the peak potentials of $[Co(PDP)_2]Cl_2.2H_2O$/GCE was investigated using cyclic voltammetry (CV). The highest peak current was observed at pH 7, compared to pH 4 and 9, demonstrating superior oxidative potential. Consequently, pH 7 buffer was selected as the electrolyte.

3.9.4. Repeatability and storage stability

To reuse the constructed working electrode, it was washed 3-4 times by dipping the AuE in a 7.5 potassium phosphate buffer solution. The assay was conducted weekly to monitor its activity over time. After 80 days of regular use, the enzyme electrode retained 85% of its initial activity, indicating that $[Co(PDP)_2]Cl_2.2H_2O$/GCE demonstrates good biocompatibility. The storage stability of the FA biosensor was evaluated over a period exceeding five months. During this time, the biosensor lost 45% of its initial activity. The working electrode was stored in a dry condition at 4°C when not in use.

Table 3. Analytical recoveries of constructed Folic acid (FA) biosensor

S.No.	FA added (nM)	FA found (nM)	% Recovery	Ref.
1	X+ null	11.0	100%	[50]
2	X+5	15.75	95%	[51]
3	X+5+5	20.65	97%	[52]
4	X+5+5+5	25.566	98%	[53]

X=Unknown concentration of FA in serum sample

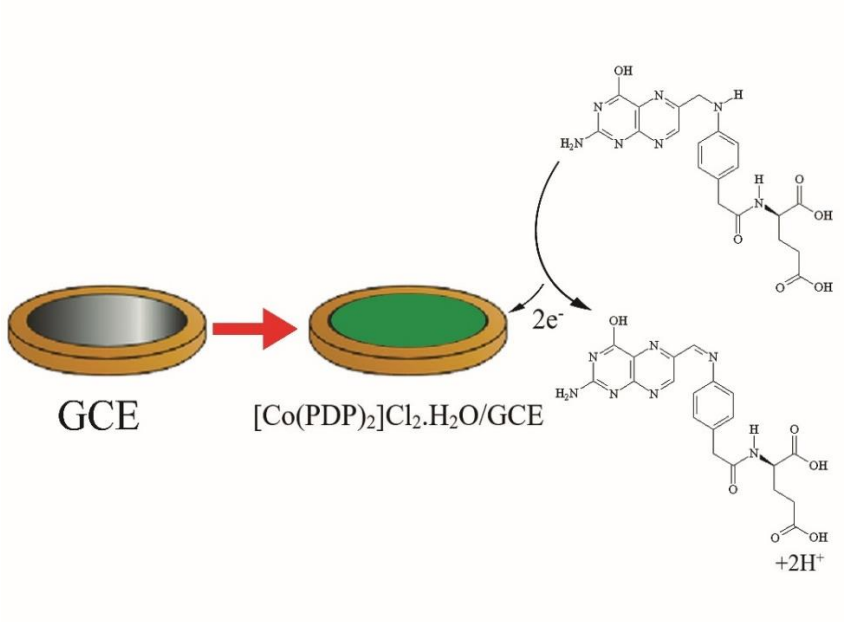

Figure 6. The mechanism for electrooxidation on the electrode surface for Folic acid (FA)

3.9.5. The mechanism for electrooxidation on the electrode surface of folic acid

The mechanism of electrooxidation on an electrode surface is a complex interplay of electron transfer, mass transport, surface interactions and reaction kinetics. All such reactions are influenced the properties of the electrode and the surrounding environment. Understanding these factors is crucial for optimizing and controlling electrochemical processes in various applications. It was observed most probably that reversible electron loss from folic acid occur on the surface of the modified electrode leading to the formation of Schiff base product. The probable reaction mechanism on the surface of modified electrode [54,55] is shown in Figure 6. The comparison of electrode sensitivity, limit of detection (LOD) and Linearity is provided in Table 4. The modified electrode utilized in this study demonstrated enhanced sensitivity for Folic acid detection in solution compared to previously reported studies. Additionally, the results indicated a slightly higher limit of detection along with an extended linear range.

Table 4. Comparison of analytic parameters for modified electrodes used for folic acid determination

Modified electrode	**Electroanalytical techniques employed**	**Linear range (µM)**	**LOD (µM)**	**Ref.**
Gold nanoparticle and graphene modified carbon ionic liquid electrode	CV, DPV	0.01-50	2.7	[56]
Mn doped SnO_2 nanoparticles (NPs) modified GCE	EIS, CV and SWV	1-500	3.8	[57]
DNA modified-pencil graphite electrode	SWV, DPV	0.1-10.0	1.06×10^{-5}	[58]
$[Co(PDP)_2]Cl_2.2H_2O$/GCE	CV	0.9953	0.0666	This work

Table 5. Analytical parameters for CV for modified electrodes used for folic acid determination

Electrode material	**Methods**	**Linear range (µM)**	**Sensitivity**	**LOD (µM)**	**Ref.**
AuNP@CuONW/Cu_2O/CF	CV	2.8-2000	1.619	0.9	[59]
CuO/PANI-NF-FTO	CV	0.25-4.6	1.359	0.24	[60]
CNT fiber	CV	0.0015-0.098	0.308	0.38	[61]
$[Co(PDP)_2]Cl_2.2H_2O$/GCE	CV	0.9953	3.507	0.0666	This work

The comparison of different electrodes in terms of their sensitivity, limit of detection (LOD), and linearity used CV method was done in Table 5. The cyclic voltammetry analysis demonstrates that the electrode used in this study has a higher sensitivity for detecting folic acid than those reported in previous studies. Additionally, although the limit of detection is

slightly higher, the linear range of detection is wider, indicating a better performance in detecting varying concentrations of folic acid.

3.10. Results and Discussion of Biological Evaluation

3.10.1. Antimicrobial activity

The antibacterial activity of the synthesized compounds is tested against four bacterial and two fungal strains at two different concentrations (100 & 200 g/mL), and it is found that the metal complexes are more effective than the free ligand. The results are present in Table 6 and showed in supplementary Figures S11 and S12. When compared to other complexes and uncoordinated ligand in similar experimental procedure, PDP-1 and PDP-2 display good biological activity for all the investigated bacterial and fungal species. The remarkable biological activity demonstrated by PDP-1 and PDP-2 is fully elucidated by chelation theory and overtones concept [62]. Cell permeability refers to the lipid membrane covered the cell that allows only lipid soluble materials to flow. Liposolubility play an important role in the control of antimicrobial activity. Chelation significantly changes the polarity of a metal ion because it partially shares its positive charge with the donor groups and improves the displacement of p and d- electrons over the entire chelate ring. The lipophilic nature of the central atom could be increased by such a chelation, resulting in the permeation of the ligand through the cell membrane lipid layer. Further MIC studies were performed for ligand (and ligand complexes) against bacterial strains as well as fungal strains, where Cu(II) and Co(II) complexes showed potential values compared to free ligand (and other metal complexes). The relative data for MIC are included in Table 6.

Table 6. Antimicrobial activity of PDP and its metal complexes (Inhibition zone in mm)

Comp. No.	**Antifungal activity**				**Antifungal activity**			
	S. aureus		***E. coli***		***A. flavus***		***P. anomala***	
	100	200	100	200	100	200	100	200
PDP	11.55 ± 2.87	14.66 ± 0.57	9.66 ± 1.15	13.66 ± 1.57	8.66 ± 0.33	12.66 ± 0.67	7.66 ± 1.47	11.66 ± 2.57
PDP-1	9.33 ± 0.57	13.54 ± 0.57	11.76 ± 0.57	12.66 ± 1.57	10.36 ± 1.57	11.66 ± 0.33	9.66 ± 0.33	12.66 ± 1.57
PDP-2	10.43 ± 2.76	12.56 ± 1.32	10.66 ± 0.98	13.36 ± 0.57	10.66 ± 0.57	12.66 ± 0.90	11.66 ± 0.98	12.45 ± 0.34
PDP-3	12.66 ± 0.57	15.66 ± 0.78	12.43 ± 1.15	14.33 ± 0.45	11.33 ± 1.57	14.66 ± 0.57	10.33 ± 1.15	14.33 ± 1.15
Std 1	8.66 ± 0.57	13.66 ± 0.57	11.66 ± 0.57	13.33 ± 0.57	-	-	-	-
Std 2	-	-	-	-	9.66 ± 0.57	13.33 ± 0.57	12.66 ± 0.57	14.33 ± 0.57

*Std 1: Ampicillin Std 2: Fluconazole

3.10.2. Antidiabetic activity

The synthesized PDP and its metal complexes examine for antidiabetic studies. Alpha amylase and Alpha Glucosidase are enzymes manage the stage of insulin and glucose level in blood over a long period and also control the risk of hyperglycemia. Percentage of inhibition of Alpha amylase and Alpha Glucosidase with different concentrations are tabulated in Tables 7 and 8, and Figures 7 and 8. Further, antidiabetic studies were conducted for ligand and its metal complexes against Alpha amylase and Alpha Glucosidase. Where PDP-2 and PDP-3 complexes showed more % of inhibition values compared to ligand and standard [63-65]

Table 7. Antidiabetic activity of the ligand and their metal complexes (Alpha amylase)

Comp. No.	**Alpha amylase inhibitory activity in %**			
PDP	25µg/mL	25µg/mL	25µg/mL	25µg/Ml
PDP-1	13.68	13.68	13.68	13.68
PDP-2	14.43	14.43	14.43	14.43
PDP-3	13.77	13.77	13.77	13.77
STD	14.88	14.88	14.88	14.88

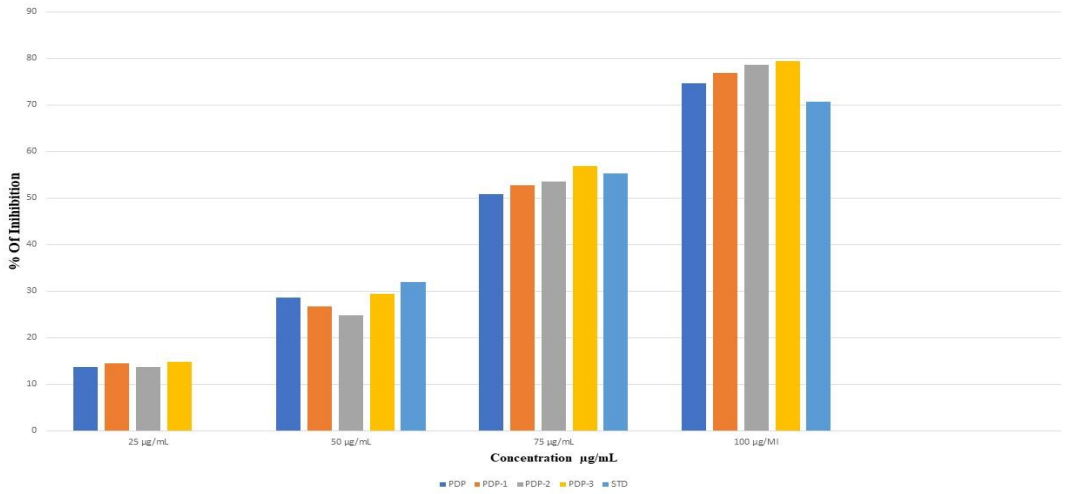

Figure 7. Alpha amylase inhibitory activity in %

Table 8. Antidiabetic activity of the ligand and their metal complexes (Alpha Glucosidase)

Comp. No.	**Alpha Glucosidase inhibitory activity in %**			
PDP	**25µg/mL**	**25µg/mL**	**25µg/mL**	**25µg/mL**
PDP-1	17.61	17.61	17.61	17.61
PDP-2	14.43	14.43	14.43	14.43
PDP-3	13.77	13.77	13.77	13.77
STD	14.30	14.30	14.30	14.30

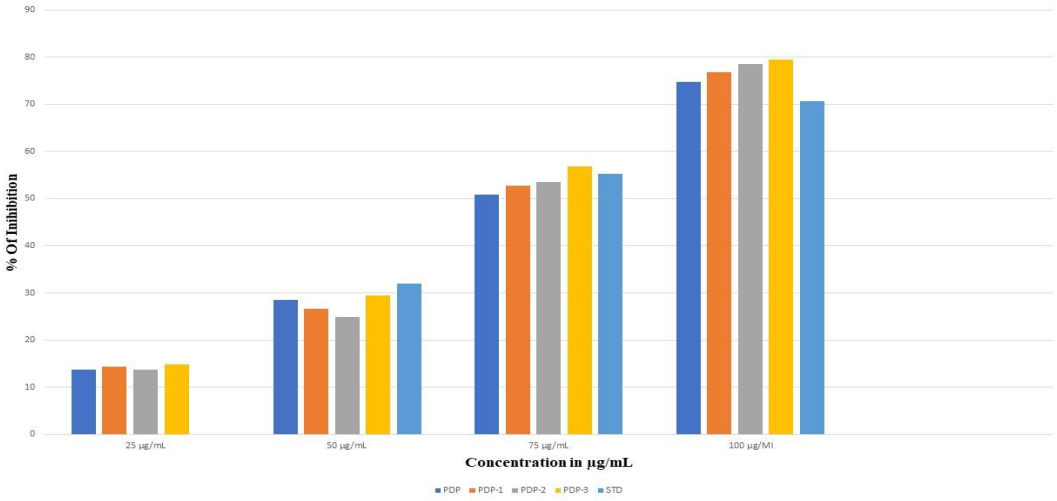

Figure 8. Alpha glucosidase inhibitory activity in %

3.10.3. IC_{50} Method

The antidiabetic activity for the synthesized ligand its metal complexes are carried out as per IC_{50} method discussed in the procedure section. The activity was screened for Alpha amylase and Alpha Glucosidase enzymes and results are indexed in Table 9 and represented supplementary Figure S13. PDP-3 and PDP-2 complexes displayed potential values in comparison with that of ligand and standard [66,67].

Table 9. IC_{50} value of PDP and their metal complexes against an alpha-amylase and alpha-Glucosidase antidiabetic activity in µg/mL

Comp. No.	**IC_{50} value in µg/mL (alpha-amylase)**	**IC_{50} value in µg/mL (alpha-Glucosidase)**
PDP	90.7082	72.01198
PDP-1	103.6590	101.5234
PDP-2	105.3456	103.2230
PDP-3	99.21781	107.1575
STD	37.12314	26.7369

4. CONCLUSION

The novel ligand, 4-[(*E*)-(3-hydroxypyridin-2-yl)diazenyl]-5-methyl-2-phenyl-2,4-dihydro-3*H*-pyrazol-3-one (PDP) was synthesized and using the synthesized ligand the biologically active Co, Ni and Cu complexes were synthesized. The structure of the ligand and its complexes were determined by using a various physicochemical and spectroscopic methods. This synthetic technique indicated the development of metal complexes in the molar ratio 1:2 (Metal:Ligand). These complexes were uni-bivalent according to molar conductance study and are tridentate in nature. The structure of synthesized metal complexes proposed to have

octahedral geometry. The electrocatalytic activity of the $[Co(PDP)_2]Cl_2.2H_2O$/GCE towards different concentration of FA was determined while showed very good results which high sensitivity, lower limit of detection (LOD). The bio-efficacy of antimicrobial and antidiabetic activity of the uncoordinated ligand its metal complexes were examined. The results of that antimicrobial activity indicated that Cu(II) and Ni(II) complexes exhibited fairly good activity while the Co(II) complex showed moderately good active, similarly the results of antidiabetic activity showed excellent activity for the Cu(II) and Ni(II) complexes.

Declarations of interest

The authors declare no conflict of interest in this reported work.

REFERENCES

[1] N. Ranjitha, G. Krishanamurthy, M.N. Manjunath, H.S. Bhojya Naik, M. Pari, N.K. Vasanthkumarnaik, J. Lakshmikantha, and K. Pradeep, J. Mol. Struct. 1274 (2023) 134483.

[2] N. Venugopal, G. Krishnamurthy, H. S. Bhojya Naik, and P. Muruli Krishna, J. Mol. Struct. 1183 (2023) 37.

[3] N.S. Kumar, G. Krishnamurthy, D. Yadav Bodke, H. Vikas Malojirao, T.R. Ravikumar Naik, S. Kandagalla, and B.T. Prabhakar, New J. Chem. 43 (2019) 790.

[4] N. Sunil Kumar, G. Krishnamurthy, Madhusudana somegowda, Maltesh Pari, T. R. Ravikumar Naik, K. S. Jithendra Kumar, Satish Naik, S. Kandagalla, and N. Naik, J. Mol. Struct. 128586 (2020) 1220.

[5] A.J. Abadi, S. Mirzaei, M.K. Mahabady, F. Hashemi, A. Zabolian, F. Hashemi, P. Raee, S. Aghamiri, M. Ashrafizadeh, A.R. Aref, R.M. Hamblin, K. Hushmandi, A. Zarrabi, and G. Sethi, Phytother. Res. 36 (2021) 189.

[6] P. Senthil Kumar, G.J. Joshiba, C. Carolin Femina, P. Varshini, S. Priyadharshini, M. A. Karthik, and R. Jothirani, Desalination and Water Treatment. 172 (2019) 395.

[7] L. Cottet, C.A.P. Almeida, N. Naidek, M.F. Viante, M.C. Lopes, and N.A. Debacher, Appl. Clay Sci. 95 (2014) 25.

[8] J. Khalid AL-Adilee, K. Ahmed Abass, and M. Taher, J. Mol. Struct. 1108 (2016) 378.

[9] Z.S. Kouser, M. Joythi, A. Bushra Begum, M.S. Asha, F.H. Al-Ostoot, D.P. Lakshmeesha, R. Ramu, and S.A. Khanum, Results Chem. 5 (2016) 100650.

[10] A.G. Prashantha, R.A.S. Ali, and J. Keshavayya, Inorg. Chem. Commun. 127 (2016) 108392.

[11] J.A. Shimshoni, S. Soback, O. Cuneah, A. Shlosberg, and M. Britzi, J. Vet. Diagn. 25(6) (2013) 736.

[12] C.R. Sahoo, J. Sahoo, M. Mahapatra, D. Lenka, P.K. Sahu, B. Dehury, R.N. Padhy, and S.K. Paidesetty, Arab. J. Chem. 14 (2013) 102922.

[13] R. Abdizadeh, F. Hadizadeh, and T. Abdizadeh, Mol. Divers. 26 (2022) 1053.
[14] M.Z. Hassan, H. Osman, M.A. Ali, and M.J. Ahsan, Eur. J. Med. Chem. 123 (2016) 236.
[15] S. Emami, and S. Dadashpour, Eur. J. Med Chem. 102 (2015) 611.
[16] M. Juri Timonen, M. Riina Nieminen, Outi Sareila, Antonis Goulas, J. Lauri Moilanen, M. Haukka, P. Vainiotalo, E. Moilanen, and H.P. Aulaskari, Eur. J. Med. Chem. 46 (2011) 3845.
[17] H.R. Zare, N. Nasirizadeh, and M.M. Ardakani, J. Electroanal. Chem. 577 (2005) 25.
[18] P. Manivel, M. Dhakshnamoorthy, A. Balamurugan, N. Ponpandian, D. Mangalaraj, and C. Viswanathan, RSC Adv. 3 (2013) 14428.
[19] E. Jason Camp, B. Simbarashe Nyamini, and J. Fraser Scott, RSC Med. Chem. (2020). 11 (2020) 111.
[20] M.B. Sanna Jilani, M. Pari, K.R. Venugopala Reddy, and K.S. Lokesh, Microchem. J. 147 (2019) 755.
[21] N. Rajesh Hegde, B.E. Kumar Swamy, P.N. Shetti, and T.S. Nandibewoor. JEAC 635 (2009) 51.
[22] S. Deepa, B.E. Kumar Swamy, and K. Vasantakumar Pai, J. Sens. 1 (2020) 100033.
[23] H. Cheshideh, and F. Nasirpouri, JEAC 797 (2017) 121.
[24] P.C. Mandal. NISCAIR-CSIR, India (2002).
[25] M.P. Malathesh, N.Y. Praveen Kumara, B.S. Jilani, C.D. Mruthyunjayachari, and K.R. Venugopala Reddy, Heliyon (2019) 5.
[26] B.N. Chandrashekar, B.E. Kumara Swamy, K.J. Gururaj, and C. Cheng, J. Mol. Liq. 231 (2017) 379.
[27] S.B. Tanuja, B.E. Kumara Swamy, and K. Vasantakumar Pai, Electroanal. Chem. J. 798 (2017) 17.
[28] M. Pari, K.R. Venugopala Reddy, and K.B. Chandrakala, Sens. Actuator A Phys. 316 (2020) 112377.
[29] P. Malathesh, and K.R. Venugopala Reddy, J. Inorg. Organomet. Polym. Mater. 30 (2020) 3511.
[30] N. Ranjitha, G. Krishnamurthy, H.S. Bhojya Naik, Maltesh Pari, Lubna Afroz, K.R. Sumadevi, and M.N. Manjunath, Inorganica Chim. Acta. 543 (2022) 121191.
[31] N. Ranjitha, G. Krishnamurthy, H.S. Bhojya Naik, Malathesh Pari, H.A. Anilkumar, G.Y. Akarsh, and N. K. Vasantakumarnaik, Polyhedron 253 (2024) 116909.
[32] N.M. Mallikarjuna, J. Keshavayya, M.R. Maliyappa, R.A. Shoukat Ali, and Talwar Venkatesh, J. Mol. Struct. 03 (2018) 94.
[33] G.A. Mahmoud Saleh, A. Wael El-Sayed, M. Ehab Zayed, Mohamed Shawky, and G.G. Mohamed. Appl. Organomet. Chem. 38 (2024) e7397.
[34] N. Venugopal, G. Krishnamurthy, H.S. Bhojya Naik, and M. Giridhar. J. Mol. Struct. 1191 (2019) 85.

[35] A. Babakhanian, S. Kaki, M. Ahmadi, H. Ehzari, and A. Pashabadi, Biosens. Bioelectron. 60 (2014) 185.
[36] B. Batra, V. Narwal, V. Kalra, M. Sharma, and J.S. Rana. Process Biochem. 92 (2020) 343.
[37] G. Chavez-Esquivel, H. Cervantes-Cuevas, L. F. Ybieta-Olvera, M. T. Castañeda Briones, Dwight Acosta, and J. Cabello. Mater. Sci. Eng. C. 123 (2021) 111934.
[38] S. Abirami, M. Priyalakshmi, A. Soundariya, V. Antony Samrot, S. Saigeetha, R. Renitta, R. Emilin, Dhiva, and S. L. Inbathamizh. CRGSC 4 (2021) 100089.
[39] E. Vidhya, S. Vijayakumar, S. Rajalakshmi, S. Kalaiselvi, and P. Pandiyan. Acta Enol. Sin. 40 (2019) 214.
[40] S. Poovitha, M.S. Sai, and M. Parani, J. Funct. Foods 33 (2017) 181.
[41] N. Alam, and K.R. Sharma, AJPCR (2020) 13.
[42] A. José. Gutiérrez-González, A. Pérez-Vásquez, R. Torres-Colín, M. Rangel-Grimaldo, D. Rebollar-Ramos, and R. Mata, J. Nat. Prod. 84 (2021) 1573.
[43] G. Krishnamurthy, and N. Shashikala, J. Serb. Chem. Soc. 74 (2009) 1085.
[44] B.R. Kirthan, M.C. Prabhakara, H.S. Bhojya Naik, P.H. Amith Nayak, and E. Indrajith Nai, CDC 29 (2020) 100506.
[45] L. Kumar, P. Kumar, A. Narayan, and M. Kar. Int. Nano Lett. 3 (2013) 1.
[46] B. Bouzerafa, D. Aggoun, Y. Ouennoughi, A. Ourari, R. Ruiz-Rosas, E. Morallon, and M. Mubarak. J. Mol. Struct. 1142 (2017) 48.
[47] L.A. Juliard, and H. Shalit, J. Electrochem. Soc. 110(9) (1963) 1002.
[48] F. Miomandre, P. Audebert, K. Zong, and J.R. Reynolds, Langmuir 19 (2003) 8894.
[49] M. Sunjuk, L. Al-Najjar, M. Shtaiwi, B. El-Eswed, M. Al-Noaimi, L. Al-Essa, and K. Sweiden. Inorganics. 10 (2022) 43.
[50] M. Alizadeh, M. Mehmandoust, O. Nodrat, S. Salmanpour, and N. Erk. J. Food Meas. Charact. 15 (2021) 5622.
[51] D. Sangamithirai, S. Munusamy, V. Narayanan, and A. Stephen. Mater. Sci. Eng. C 91 (2018) 512.
[52] M. Abdul Mumit, T. Kumar Pal, M.A. Alam, M. Al-Amin-Al-Azadul Islam, S. Paul, and M.C. Sheikh. J. Mol. Struct. 1220 (2020) 128715.
[53] S. Pakapongpan, J.P. Mensing, D. Phokharatkul, T. Lomas, and A. Tuantranont. Electrochim. Acta 133 (2014) 294 .
[54] D. Manoj, D. Ranjith Kumar, and J. Santhanalakshmi. App. NanoSci. 2 (2012) 223.
[55] S. Akbar, A. Anwar, and Q. Kanwal. Anal. Biochem. 510 (2016) 98.
[56] X. Wang, Z. You, Y. Cheng, H. Sha, G. Li, H. Zhu, and W. Sun, J. Mol. Liq. 204 (2015) 112.
[57] N. Lavanya, E. Fazio, F. Neri, A. Bonavita, S.G. Leonardi, G. Neri, and C. Sekar, J. Electroanal. Chem. 770 (2016) 23.

[58] L. Mirmoghtadaie, A.A. Ensafi, M. Kadivar, and P. Norouzi, Mater. Sci. Eng. C 33 (2013) 1753.
[59] Z. Zhao, Q. Li, Y. Sun, C. Zhao, Z. Guo, W. Gong, J. Hu, and Y. Chen, Sens. Actuators B 345 (2021) 130379.
[60] A. Esmaeeli, A. Ghaffarinejad, A. Zahedi, and O. Vahidi, Sens. Actuators B 266 (2018) 294?301.
[61] K. Shen, J. Wang, Y. Shen, Y. Li, M. Guo, Z. Su, L. Lu, X. Cai, L. Chen, F. Song, X. Gao, J. Tang, and N. Ueno, Laser Photon. Rev. 15 (2021) 2100023.
[62] S. Shahrokhian, and H.R. Zare-Mehrjardi. Sens. Actuators B 121 (2007) 530.
[63] B.B. Beyene, M.A. Mihirteu, T.M. Ayana, and W.A. Yibeltal. Result Chem. 2 (2020) 100073.
[64] C.G. Kato-Schwartz, R.C.G. Corrêa, D. de Souza Lima, A. Babeto de Sá-Nakanishi, G. de Almeida Gonçalves, F.A.V. Seixas, C.W.I. Haminiuk, L. Barros, I.C.F.R. Ferreira, A. Bracht, and R.M. Peralta, Food Res. 137 (2020) 109462.
[65] A. Toumi, S. Boudriga, K. Hamden, M. Sobeh, M. Cheurfa, M. Askri, M. Knorr, C. Strohmann, and L. Brieger, Bioorg. Chem. 106 (2021) 104507.
[66] R. Agada, D. Thagriki, D.E. Lydia, A. Khusro, J. Alkahtani, M.M. Al Shaqha, S.M. Alwahibi, and M.S. Elshikh, J. King Saud Univ. Sci. 33 (2021) 101342.
[67] E. Deveci, F. Çayan, G. Tel-Çayan, and M.E. Duru, Afr. J. Biotech. 137 (2021) 19.